Magnetic Bearing Design for a High Speed Rotor

E. H. MASLEN, P. E. ALLAIRE, M. A. SCOTT

Department of Mechanical and Aerospace Engineering,
University of Virginia, Charlottesville, VA, USA

P. HERMANN

Sundstrand Corporation
Rockford, IL, USA

Summary

The design of an example set of magnetic bearings for a small high speed compressor is presented. The bearings were designed to replace the fluid film bearings of an existing compressor design. Reduction of parasitic power losses due to the bearings is projected to be from the current 2 kW down to approximately 200 W.

Introduction

Magnetic bearings are beginning to see application to a broad spectrum of industrial machinery. The motives for using magnetic bearings are as varied as the machines in which they are found. In large turbomachinery, these bearings have proved attractive because they can eliminate complex lubrication systems [1]. In the petrochemical industry, canned pumps can benefit from the longevity of magnetic bearings in harsh chemical environments [2]. Rotary anode X-ray tubes have taken advantage of the ability of these bearings to operate in a vacuum [3]. For the application discussed here, the primary motive for using magnetic bearings is to reduce parasitic power losses in the bearings.

The application of magnetic bearings to small, high speed rotating machinery accentuates constraints in the design of the magnetic components which may be considered of secondary importance in larger machinery. First, the magnetic components generally must fit into a very small space. This tends to discourage the use of designs requiring complex pole structures such as is the case with many of the hybrid electro-permanent magnet designs. Further, minimum coil volume dictates high coil current densities so that providing adequate cooling for the coils may be difficult. Second, the mass added to the shaft must be minimized in order to avoid adverse effects to the shaft dynamics. As a percentage of total rotor mass, the added journal mass for magnetic bearings will typically be higher in small equipment than in large. Finally, any rotating components should, if possible, be permanently mounted to the shaft so as to minimize the eccentricity (and resulting unbalance) associated with slip fits. This is especially significant in machinery intended to operate at very high speed.

Partial funding for this work was provided by Sundstrand Corporation, the Army Research Office, and the Center for Innovative Technology of the Commonwealth of Virginia.

The purpose of this paper is to describe some of the factors which should be taken into account in the bearing analysis. No attempt is made here to investigate the detailed finite element analysis which should ultimately conclude any design project of this sort.

The example bearing design to be discussed here exemplifies this type of highly constrained problem. The machine for which the bearings were designed is a small, electrically driven compressor. It has an operating speed range of 30,000 to 70,000 RPM. The motor armature is integral with the compressor shaft and is centered between the two radial bearings whose span is 20 cm. The shaft mass is approximately 1.6 kg. Design of these bearings was somewhat complicated by the requirement that they be retrofit to an existing design, so that they had to fit within the physical envelope originally provided for fluid film bearings and the associated seals.

The actual performance specifications and design figures presented here are intended only to illustrate the considerations governing the design process. They do not precisely correspond to any bearing design actually being constructed either by the authors or their sponsors.

Nomenclature

A_g	pole face area
α	temperature coefficient of wire electrical conductivity
B_{sat}	magnetic saturation flux density
β	geometry factor: $\partial G / \partial x$
c_g	ratio of total conductor volume to total coil volume
δ	characteristic coil radius
ε	bearing derating factor
f	bearing force
G	nominal air gap between bearing stator and rotor
h_c	convection coefficient
I_b	nominal, or bias coil current: time invariant
i_p	coil perturbation current: varies with time
J	coil current density
k	coil bulk thermal conductivity
k_s	spool thermal conductivity
μ_o	magnetic permeability of free space
N	total wire turns linked by a given magnetic circuit
r_s	coil spool effective inner radius = perimeter length / 2π
r_i	coil effective inner radius
r_o	coil effective outer radius
σ_o	wire electrical conductivity at T_o
T_o	reference temperature at which wire electrical conductivity is measured
T_p	pole structure fixed temperature
T_∞	coolant free stream temperature

Design Overview

The integrated compressor/bearing design is shown in Figure 1. From a mechanical point of view, several features are of immediate interest.

The bearings are constructed in such a manner that all rotating components, i.e.: the laminated stators and the thrust disk, are permanently mounted to the shaft. Disassembly of the

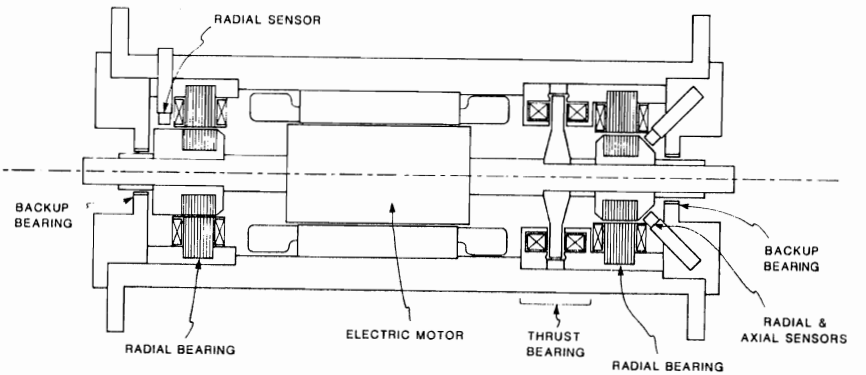

Figure 1 - Diagram of Compressor/Bearing Design

compressor does not require removal of any of these components, which permits the shaft to be balanced as an assembly outside of the compressor housing. The shaft assembly with laminated journals and thrust disk is shown in Figure 2.

Axial motion sensing can not be accomplished by simply directing a proximitor at the shaft end due to the impellers fitted to both ends of the shaft. Instead, both axial and radial motions are detected by a set of three probes at the right end of the compressor (see Figure 1.) These probes are located at ninety degree intervals around the shaft and are oriented at a forty five degree angle relative to the shaft axis. The axial, horizontal, and vertical motion of the shaft can readily be extracted from these probe signals by simple coordinate transformation. This scheme will inevitably lead to some crosstalk between the three axes due to calibration error and drift in the probes, but these effects are expected to be relatively minor.

The top shaft speed of 70,000 RPM dictates that hoop stresses in the various rotating components generated by the high centripetal forces cannot be neglected. Particularly affected by this is the thrust disk because it has the largest diameter of any of the rotating parts and also because it is constructed entirely of magnet iron, which has a substantially lower yield stress than do high strength steels. The design solution to this problem involves providing the thrust

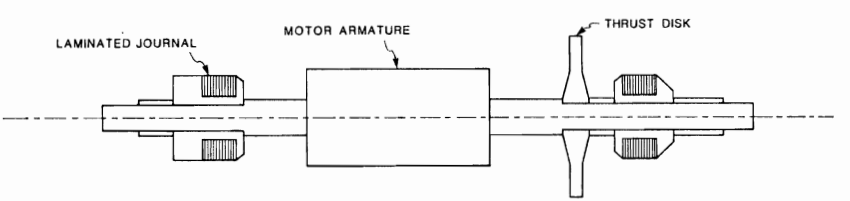

Figure 2 - Shaft with Laminated Journals and Thrust Disk

disk with a thick hub and tapering the disk to a thin section at the outer radius.

Backup bearings are provided at each shaft end in the event that the bearings should fail or an external load exceeding the capacity of the bearings should be applied. These are simple overbored bushings and are not intended for continuous operation. An axial backup bearing is provided by coating the faces of the thrust bearing with an anti-wear coating.

Performance Specification

The design of the magnetic components was guided by three major concerns: load capacity, thermal performance, and size. The radial and thrust actuators must be able to generate the magnetic forces required to meet the specified load requirements. At the same time, resistive heating in the coils must not exceed the capacity of a realistic cooling system to prevent overheating and failure of the coil insulation. Above all, any usable design must fit into the allotted space.

For the thrust bearing, the anticipated static axial force due to the pressure differential between the two stages is approximately 35 N. An additional sinusoidal component due to fluid forces generated by off-design operation of the impeller- volute interaction is expected to be on the order of ten percent of the static load. Excess load capacity of three times the total shaft weight, or 48 N is required for transient loads.

The radial bearings must support the static weight of the shaft (about 8 N per bearing) plus unbalance forces and transient loads. Impeller blade pass and hydrodynamic unbalance forces are expected to be substantially smaller than mass unbalance effects. The largest synchronous harmonic forces to be generated by the magnetic bearings depend both on the worst case unbalance distribution and the control algorithm employed. For the initial design work, it was assumed that these forces would be at most 4 N. The transient loads are expected to be no more than three times the rotor weight, or 24 N.

Cooling of the coils is provided by two primary mechanisms: conduction to the pole structure and convection to a cooling fluid. The thrust bearing coil is entirely enclosed by the pole structure and the thrust disk, so that only conduction to the pole structure is significant for this coil. For the radial bearings, however, the coils are exposed to the working fluid, so they can be convectively cooled as well. As design limitations for these two mechanisms, it was assumed that the temperature of the pole structure would not exceed 60°C and that the maximum allowable coolant flow rate is about 800 cc/sec. The coolant fluid is air at a maximum supply temperature of 50°C.

Space restrictions are the least flexible contraint in the problem. The outer diameter of the motor armature sets the minimum inner radius of the thrust bearing at 1.9 cm. If the thrust bearing pole pieces are of a smaller inner radius then disassembly of the compressor will require removal of the thrust disk. The casing dimensions fix the maximum outer diameter of both the thrust and radial bearings at 7.0 cm. Finally, the axial length of the thrust and radial bearing set on the right end of Figure 1 could not exceed 6.5 cm.

Magnetic Model

For each of the five axes of control, an axially opposed pair of electro- magnet pole structures as shown in Figure 3 provides a reversible control force. The magnet coils are energized with a fixed bias current of equal magnitude on each side. The coil currents are then symmetrically perturbed to produce the dynamic control force. The fixed bias current provides a limited linearization of the bearing force - perturbation current relationship, as well as permitting rapid changes in bearing force (high slew rate) even when the nominal bearing force is zero [4].

Simple analytic studies of this arrangement have been widely reported in the literature [5,6]. The analysis yields an analytic expression relating the bearing force to the various design parameters but neglects nonideal behavior of the magnetic circuit such as leakage and fringing. Allaire, et al. [2] have proposed a fairly simple scheme for computing a correction factor, ε, which derates the bearing performance based on an approximate calculation of the permeabilities of the leakage and fringing paths. The derating factor is fairly insensitive to small changes in design geometry so that various designs may be compared using the same derating factor. A factor of 1.1 was used for both the radial and thrust bearings at the design stage.

The resulting governing equation is:

$$f = \frac{\mu_o \beta N^2 A_g}{4\varepsilon^2}\left[\frac{{i_1}^2}{(G-\beta x)^2} - \frac{{i_2}^2}{(G+\beta x)^2}\right]$$

where the currents i_1 and i_2 are governed and restricted by

$$i_1 = I_b + i_p, \quad 0 \le i_1 \le i_{sat} \qquad i_2 = I_b - i_p, \quad 0 \le i_2 \le i_{sat}$$

and i_{sat} is the coil current which produces magnetic saturation in the pole structure:

$$i_{sat} = 2GB_{sat} / \mu_o N\varepsilon$$

Thermal Model

The ultimate goal of thermal models in magnetic bearing design is to determine the maximum wire temperature within the coil as a function of the coil current. This maximum temperature must be less than the manufacturer's thermal rating for the wire insulation.

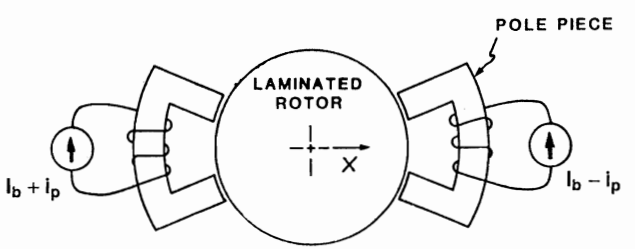

Figure 3 - Actuator Current Configuration

In this study, an analytic thermal model of the coils was used to predict the maximum wire temperature. This model is based on the following approximations:

1. the coil thermal conductivity can be modeled as a homogeneous bulk property
2. the coil geometry is adequately modeled as cylindrical
3. thermal gradients are purely radial
4. convection from the coil outer surface is uniform
5. the coil is wound on a spool of finite conductivity
6. the spool is in intimate contact with a pole piece at fixed temperature at its inner radius (a low spool conductivity can be used to simulate high contact resistance)
7. the electrical conductivity of the coil wire varies with temperature according to $\sigma = \sigma_o/(1+\alpha[T-T_o])$, where σ_o is the nominal conductivity measured at the temperature T_o: $\alpha = 0.00393/°C$ for copper wire, $\sigma(T=20°C) = 5.8\times10^6$ mho/cm

Given these approximations, the temperature in the coil can be represented by

$$T(r) = \tau c_1 J_o(r/\delta) + \tau c_2 Y_o(r/\delta) + T_o - 1/\alpha$$

where $\delta \equiv [(\sigma_o k c_g)/\alpha]^{1/2}/J$, $\tau \equiv T_\infty - 20 + 1/\alpha$, $\tau_p \equiv (T_p - 20 + 1/\alpha)/\tau$, J_o and Y_o are zero order Bessel's functions of the first and second kind, and the coefficients c_1 and c_2 are found from the matrix equation

$$\begin{bmatrix} \dot{J}_o(r_o/\delta) + h_c\delta J_o(r_o/\delta)/k & \dot{Y}_o(r_o/\delta) + h_c\delta Y_o(r_o/\delta)/k & 0 \\ \dot{J}_o(r_i/\delta) & \dot{Y}_o(r_i/\delta) & -\delta k_s/k r_i \\ J_o(r_i/\delta) & Y_o(r_i/\delta) & ln(r_s/r_i) \end{bmatrix} \begin{bmatrix} c_1 \\ c_2 \\ c_3 \end{bmatrix} = \begin{bmatrix} h_c\delta/k \\ 0 \\ \tau_p \end{bmatrix}$$

Smith [7] provides a table originally developed by General Electric which correlates a conductivity enhancement factor (to be applied to the conductivity of the coil potting compound) with the percent metal by volume of the coil. For a typical wire packing factor of 0.72, the coil is about 57% metal by volume. Assuming full impregnation of the coil with polyester potting compound, the bulk conductivity of the coils should be about 0.012 W/cm/°C.

Given the specified limit on coolant flow rate and an estimate of the free space between the coils, the coolant free stream velocity around the radial bearing coils is expected to be on the order of 4 m/sec. The convection coefficient can be computed using standard expressions for multitube heat exchangers [8]. The predicted convection coefficient is 0.008 W/cm^2 /°C.

Assumption 1 produces a model which does not indicate the local thermal gradients surrounding the individual conductors, while assumptions 3 and 4 ignore stagnation zones in the coolant flow. Further, the thrust bearing coil is in contact with the pole structure both on its inner radial surface and on one of its axial faces (see Figure 1.) This additional conduction cooling is ignored by assumptions 3 and 6. Because of these three significant errors, the model can be expected to predict peak temperatures which are low for the radial coils and probably a little high for the thrust coils.

With the exception of coolant stagnation, these errors can be avoided by using a finite element model to compute the temperature distribution. The model must be quite detailed, however, in order to properly predict the local gradients surrounding the conductors.

The approach actually adopted in this study employed various engineering judgements in applying the coil current density limits determined by the analytic model. These judgments are discussed in the next section. The current densities arrived at in this manner appeared to be consistent with industrial experience in the design of electric motors. For both bearings, the current limits predicted by the thermal model were compared to the RMS current required to generate the stated static and harmonic load capacities.

Bearing Design

Given the close spatial limits for the bearings, the design approach was to first find the axially shortest thrust bearing design which would meet the performance requirements. The analytically determined thermal limits were followed fairly closely, with the modification that the peak coil temperature used to determine the maximum allowable current density was 40°C lower than the wire manufacturer's limit. This provided a safety margin which should accomodate localized gradients.

Once the thrust bearing design was determined, the radial bearing was designed to fill the remaining space. In this way, a thermally conservative design was obtained for the radial bearing for which the thermal model is expected to be the least certain.

Choice of the magnetic air gap length for the two bearings was somewhat arbitrary. For both bearings, a gap of 0.5 mm was used, which is twice the tolerable shaft excursion in each direction. This figure reflects a desire to limit actuator nonlinearities due to shaft displacement: a shorter gap would produce a strongly nonlinear bearing, whereas an excessively long gap produces a reduced current-to-force gain resulting in high power losses.

The resulting bearing designs are summarized below.

Thrust Bearing	
Rated RMS load	37.5 N
Peak load capacity	273.8 N
Coil current density at RMS load	465 A/cm^2
Maximum safe current density (thermal model)	640 A/cm^2
Coil resistance	3.9 Ω
Coil inductance	6.4 mH
Wire turns per coil	323
Wire gage	26
Bias coil current	0.55 A
Nominal air gap	0.05 cm
Coil thickness (axial)	0.96 cm
Coil thickness (radial)	0.76 cm
Spool Thickness	0.08 cm
Total package length (2 bearings + thrust disk)	3.57 cm
Linearized open loop stiffness	-69600 N/m
Linearized actuator gain	77.8 N/A
Radial Bearing	
Rated RMS load	10.8 N

Peak load capacity	45.1 N
Coil current density at RMS load	576 A/cm^2
Maximum safe current density (thermal model)	1270 A/cm^2
Coil resistance (per coil)	1.62 Ω
Coil inductance (per coil)	4.5 mH
Wire turns per coil	189
Wire gage	26
Bias coil current	1.30 A
Nominal air gap	0.05 cm
Journal length	1.00 cm
Journal diameter	3.50 cm
Coil length	1.18 cm
Coil thickness (radial)	0.41 cm
Spool Thickness	0.08 cm
Bearing axial length	1.80 cm
Linearized open loop stiffness	-83600 N/m
Linearized actuator gain	35.7 N/A

The axial length occupied by these two bearings is 5.4 cm out of the total 6.5 cm available. This leaves 1.1 cm for probes, coolant passages, and clearance around the motor windings in the right end bearing envelope.

Power Loss Estimates

There are three main sources of power dissipation which must be considered for magnetic bearings. These are resistive losses in the coils, inefficiency of the coil power supply and power amplifier, and combined eddy current and hysteretic losses in the magnet iron. The first are readily estimated from the expected loads, the actuator gain, and the coil resistances. For the radial bearings operating at rated RMS load, the anticipated power loss would be a total of 49.3 watts. The thrust bearing should dissipate approximately 3.9 watts at rated load.

The inefficiencies of the supporting power electronics provide a multiplicative factor for the coil current losses. For a conventional transformer-capacitor DC power supply and a pulse width modulated power amplifier, the total efficiency should be on the order of 75 percent. This raises the electrical power losses associated with each of the bearings by a factor of 1.33, yielding 65.7 watts for the radial bearings and 5.3 watts for the thrust bearing.

The hysteresis and eddy current losses are difficult to estimate accurately, but an upper bound can be determined by computing a worst case flux variation in the stator and rotor, assume that the fluctuations permeate the magnet iron uniformly, and use manufacturer's data to determine the resulting losses. For the radial bearing journal, the worst case operation would involve complete reversal of the saturation flux density in the rotor at a frequency of four times the highest running speed. This corresponds to a sinusoidal flux variation of amplitude 1.2 Tesla at a frequency of 4800 Hz. For the stator, the maximum amplitude of flux variation should be one half of the saturation density at a frequency equal to the maximum running speed. This corresponds to a sinusoidal flux variation of 0.6 Tesla amplitude at a frequency of 1200 Hz. The total magnet iron mass associated with the radial bearing pole structures is 0.232 kG, while the combined mass of the two journal laminations is 0.073 kG. Given these

figures and the manufacturer's data on iron losses for the lamination material, the expected losses are 5.1 watts in the pole pieces and 40.2 watts in the journals.

The total power losses for these bearings are thus conservatively estimated at under 200 watts. This is a reduction of at least 90% from the 2 kW reported with fluid film bearings.

Effect on Shaft Dynamics

One of the most troublesome aspects of applying magnetic bearings to small flexible rotors is that significant rotating mass must be added to the rotor in the form of laminated journals and the thrust disk. This tends to reduce the frequencies of the higher critical speeds and may bring them into the operating range. Figure 4 shows the critical speed map of this rotor prior to addition of the magnetic bearing components. The operating speed range is neatly tucked in between the third and fourth critical speeds, providing an acceptable speed margin at both of the extremes. After adding the magnetic components, Figure 5 shows that the fourth critical speed has been dropped into the upper extreme of the operating range. If the bearing is capable of providing sufficient damping at this speed, then this condition will be acceptable although not desirable. For such a design, rigorous analysis of the unbalance response near the fourth critical is mandated.

Conclusions

The magnetic component design for magnetic bearings in a typical high speed rotor has been presented. Three primary design factors were considered: load capacity, thermal performance, and size. The relations presented for analyzing the design are approximate, but are useful in the preliminary design stage. Any bearing design should ultimately be examined using finite element methods.

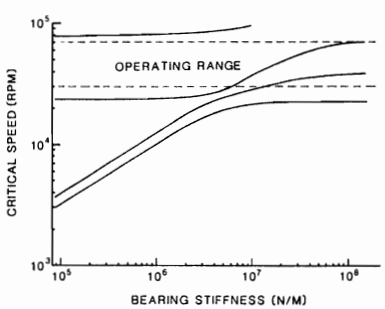

Figure 4 - Critical Speed Map of Original Rotor

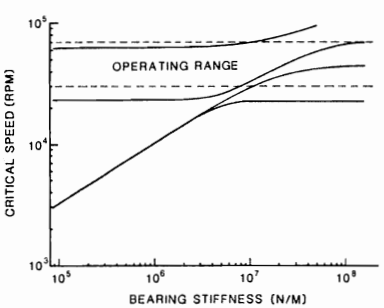

Figure 5 - Critical Speed Map with Magnetic Bearing Components

To date, very few magnetic bearings have been employed in high speed rotors. Much research and design work needs to be done to make the design procedure as routine as it is for more conventional bearings. The development of computer programs using the type of analysis presented in this paper will greatly assist in this process. Advanced finite element packages will also be required and are beginning to emerge. In particular, there is a need for a method of estimating eddy current and hysteretic losses which is more convenient than the detailed analyses currently in the literature, but more accurate than the very crude method desribed in this paper.

References

1. Foster, E. G., V. Kulle, and R. A. Peterson. "The Application of Active Magnetic Bearings to a Natural Gas Pipeline Compressor". ASME paper 86-6T-61.

2. Allaire, P.E., A. Mikula, B. Banerjee, D.W. Lewis, and J. Imlach. "Design and Testing of a Magnetic Thrust Bearing". Proceedings of the NASA Workshop on Magnetic Bearings, Langley, VA, March 1988.

3. Sudo, H. and A. Takahashi. "Rotary Anode X-Ray Tube". Patent No. 4468801, issued Aug. 28,1984. assignee: Toshiba Corp.

4. Maslen, E., P. Hermann, M. Scott, and R. Humphris. "Practical Limits to the Performance of Magnetic Bearings: Peak Force, Slew Rate, and Displacement Sensitivity". Proceedings of the NASA Workshop on Magnetic Bearings, Langley, VA, March 1988.

5. Hebbale, K.V. "A Theoretical Model for the Study of Nonlinear Dynamics of Magnetic Bearings." Doctoral Dissertation, Cornell University, Ithaca, N.Y., USA, January, 1985.

6. Schweitzer, G. and R. Lange. "Characteristics of a Magnetic Rotor Bearing for Active Vibration Control", Technishe Universitat Munchen, Institut fur Mechanik, IMECHE 1976.

7. Smith, S. *Magnetic Components Design and Applications*. Van Nostrand Reinhold, New York, p.172.

8. Kreith, F. *Principles of Heat Transfer*. Harper and Row, New York, 1973. p.487.

Vibration Control of Flexible Rotors